

Band-gap renormalization in quantum wires

R. Cingolani,* R. Rinaldi, and M. Ferrara

Dipartimento di Fisica, Università di Bari via Amendola 173, 70110 Bari, Italy

G. C. La Rocca

Scuola Normale Superiore di Pisa, Piazza dei Cavalieri 7, 56100 Pisa, Italy

H. Lage,[†] D. Heitmann,[‡] and K. Ploog[§]

Max-Planck-Institut für Festkörperforschung, Heisenbergstrasse 1, D7000-Stuttgart 80, Federal Republic of Germany

H. Kalt

University of Kaiserslautern, Fachbereich Physik, Federal Republic of Germany, E. Schrödinger Strasse, D-6750 Kaiserslautern, Federal Republic of Germany

(Received 2 November 1992; revised manuscript received 8 March 1993)

The carrier density dependence and the temporal evolution of the ground level parameters of a quasi-one-dimensional electron-hole plasma confined in GaAs quantum wires have been studied by a line-shape analysis of the time-resolved luminescence. The obtained data are compared with the available theoretical calculations.

I. INTRODUCTION

When a dense electron-hole plasma (EHP) forms in a semiconductor, the single-particle picture breaks down and the crystal ground level differs from the one calculated for noninteracting electron-hole pairs. The progressive shrinkage of the band gap with increasing EHP density is one of the macroscopic consequences of many-body interactions in the crystal. This phenomenon, known as band-gap renormalization (BGR), is important to forecast the emission wavelength of coherent emitters, and has been widely studied in recent years in semiconductors of different dimensionalities.¹ Most of the work has been aimed to a quantitative determination of the carrier density dependence of the BGR in bulk as well as in quantum well semiconductors. The dimensionality dependence of the BGR has also been demonstrated. In this work we present an experimental investigation of band gap renormalization in a hot-carrier plasma photo-generated by short laser pulses in GaAs quantum wires. The carrier density dependence and the time evolution of the BGR and of the carrier temperature have been obtained by the line-shape analysis of the time-resolved photoluminescence (PL) of highly excited quantum wires.

II. EXPERIMENTAL

The investigated quantum wire array was fabricated by holographic lithography and plasma etching from a GaAs/Al_{0.36}Ga_{0.64}As multiple quantum well heterostructure (the well and barrier widths were 10.6 and 15.3 nm, respectively). The resulting quantum wires had a lateral width of 60±5 nm. Details on the investigated structure are reported in Refs. 2 and 3. The sample was kept at a lattice temperature of 5 K and optically excited by the second harmonic of a mode-locked Nd:Yag (yttrium

aluminum garnet) laser with pulse duration of about 25 ps and repetition frequency of 2 Hz. The temporal evolution of the luminescence was analyzed by a single-shot streak-camera equipped with a cooled charge coupled device detector.

III. RESULTS AND DISCUSSION

In Fig. 1 we show the high-excitation-intensity photoluminescence (PL) spectra of the quantum wires at different delays after the exciting pulse. The spectra were recorded at power densities ranging between 0.5 and 10 MW cm⁻², and measured for delay times of the order of 1 ns, until the PL signal extinguishes completely. The spectra exhibit a band-filling line-shape as usually observed for the electron-hole plasma emission of low-dimensional semiconductors. These spectra originate from the radiative recombination of electron and holes occupying quantum wire subbands with quantum numbers as high as $n_y=5$ and following the selection rule $\Delta n_y=0$ (y labels the quantum wire confinement direction).³ As shown by the vertical lines in Fig. 1, the relative positions of the PL structures reflect the energy splitting of the first five interband transitions in the wires.^{3,4} These were obtained by adding the lateral confinement energies from a Kohn-Luttinger-type calculation of the valence-band states,⁵ and from a simple square-well model calculation of the conduction bands, to the quantum well gap. The exact energy of the unperturbed $n_y=1$ energy gap of the wires (E_g) has been determined from the experimental position of the $2p$ exciton state measured by two-photon-absorption spectroscopy.⁶ For the investigated wire array we found $E_g=1.566$ eV at low temperature. In general, at short delays after the exciting pulse the PL spectra exhibit broad tails, indicating the presence of a hot-carrier distribution (high-energy tail) and band-gap renormalization (low-energy tail). With increasing

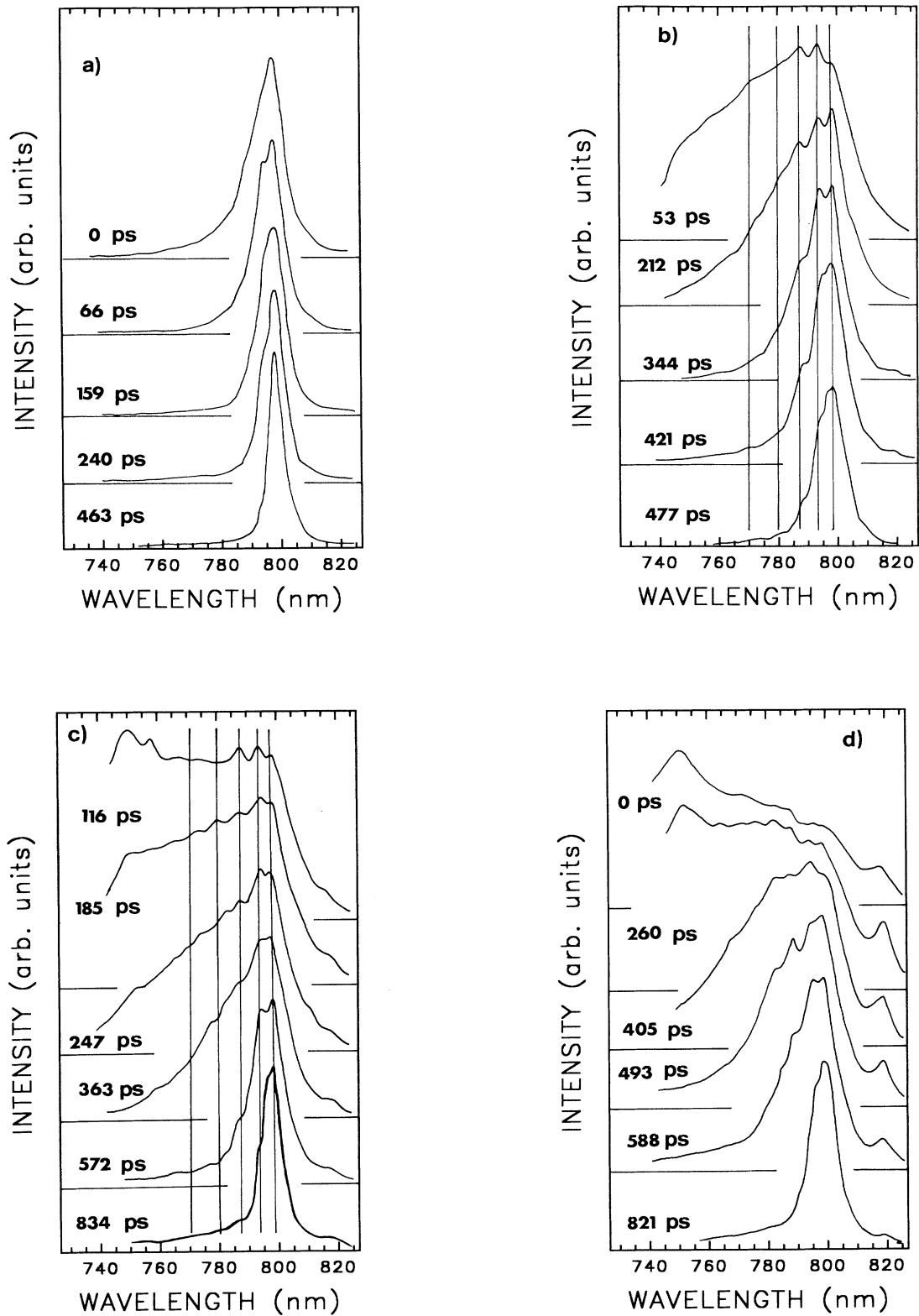


FIG. 1. Time-resolved electron-hole plasma luminescence spectra recorded under different excitation intensities: (a) $I = I_0$; (b) $I = 5I_0$; (c) $I = 10I_0$; (d) $I = 20I_0$ ($I_0 = 0.5 \text{ MW cm}^{-2}$). The vertical lines indicate the relative position of the calculated interband transitions among quantum wire states of quantum number $1 < n_y < 5$ and selection rule $\Delta n_y = 0$.

delays, energy relaxation of hot carriers occurs. The spectra narrow and distinct interband transitions become distinguishable. At long delays the PL spectrum reduces to a sharp peak with some additional structure in the high energy tail due to a residual population in the $n_y = 2$ quantum wire subbands. At the lowest excitation intensity [Fig. 1(a)] only few subbands are populated, and the luminescence spectra are narrower. With increasing excitation intensity a strong broadening of the high energy tail of the spectra is observed. The population of states belonging to the second quantum well subband and the saturation of the quantum wire density of states can be observed in the spectra of Figs. 1(c) and 1(d) at short delays. Under these conditions the luminescence persists for delays as long as 1 ns due to the relaxation of hot carriers into the lower quantum wire sub-bands. This time dynamics reflects the temporal evolution of the carrier density in the quantum wire states, which is expected to be maximum after the laser pulse and then to decrease following the e - h pair lifetime in the plasma. Following this plasma dynamics the BGR and the hot-carrier tem-

perature are expected to decrease either with decreasing the excitation intensity or with increasing the delay time after the exciting pulse. Qualitatively, a time (i.e., density) dependence of the BGR and of the carrier temperature can be inferred by the progressive narrowing of the low- and high-energy tail, respectively, observed at long delays in the PL spectra of Fig. 1.

To get quantitative information on the temporal evolution of the EHP parameters we have performed a statistical analysis of the luminescence line shape. Electrons and holes in the plasma are described by a quasi-equilibrium Fermi-Dirac distribution functions ($f_{e,h}$) with common carrier temperature (higher than the crystal temperature).⁷ This approximation is fulfilled in the time scale of our experiment, as the typical carrier thermalization time is 1 ps,⁸ whereas the recombination time is of the order of ns. Assuming that the many-body interactions modify the single particle energy states causing a rigid band shift and a quasiparticle broadening, the resulting spectral density of emission for a constant transition matrix element reads as⁹

$$I(\hbar\omega) \simeq \sum_{j=1}^N \int dE' \int dE_e \int dE_h \delta(\hbar\omega - E_e - E_h - E_g^*) \times f_e(\epsilon_{je}) f_h(\epsilon_{jh}) D(E' - E_g^* - E_{je} - E_{jh}) L_e[E_e, \epsilon_{je}(E')] L_h[E_h, \epsilon_{jh}(E')], \quad (1)$$

where the summation is over N occupied subbands, E_g^* is the normalized band gap,

$$\epsilon_{je,h} = \frac{m_{h,e}}{m_e + m_h} (E' - E_g^* - E_{je} - E_{jh}) + E_{je,h}, \quad (2)$$

consistent with the assumption of momentum conservation in the recombination, and $D(E)$ is the joint one-dimensional density of states proportional to $E^{-1/2}$. The values used for the five parabolic effective masses are $m_e = 0.067$ and $m_h = 0.2$. The latter has been chosen to reproduce on average the dispersion of the four topmost one-dimensional (1D) hole subbands.⁵ In this model the quasiparticle spectral functions are given by Lorentzian functions $L_{e,h}$ with constant damping parameters $\Gamma_{e,h}$, which account for intercarrier scattering.¹⁰ If in the Fermi-Dirac functions the approximation $E_e \simeq \epsilon_{je}(E')$ and $E_h \simeq \epsilon_{jh}(E')$ are made, Eq. (1) reduces to

$$I(\hbar\omega) \simeq \sum_{j=1}^N \int de' f_e[\epsilon_{je}(E')] f_h[\epsilon_{jh}(E')] \times D(E' - E_g^* - E_{je} - E_{jh}) L(\hbar\omega, E'), \quad (3)$$

where the Lorentzian function L has a broadening parameter $\Gamma = \Gamma_e + \Gamma_h$. Within this model, given the values of the electron and hole 1D subband edges E_{je} and E_{jh} (measured and calculated in Refs. 3 and 5), and varying the total e - h pair density (n), E_g^* , the carrier temperature T and Γ as fitting parameters, a satisfactory line-shape analysis of the spectra is obtained as shown by the typical results of Fig. 2.¹¹

The renormalized band gap falls in the low-energy tail of the PL spectra (arrows in Fig. 2) and is redshifted with respect to the $n_y = 1$ gap of the unperturbed quantum wire by an amount which depends on the excitation intensity and/or the delay time. The results of the present model do not differ much from those obtained in our previous work³ where the one-dimensional joint density of states itself was phenomenologically broadened; such an

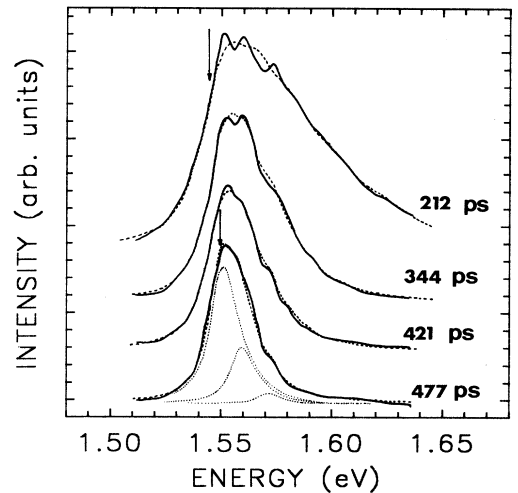


FIG. 2. Time-resolved electron-hole plasma luminescence spectra measured at 5 K (continuous lines) and calculated spectra (dashed lines). The arrows indicate the renormalized band gap. The individual interband transitions are plotted for the 477-ps spectrum.

approach would be more appropriate if the broadening were dominated by wire-width fluctuations or other defects rather than by lifetime (Landsberg-like) damping. As the typical values of Γ are comparable to those of the temperature,¹² several spectra have also been fitted using Eq. (1) in which no approximations are made in evaluating the Fermi-Dirac distribution functions. The (unphysical) low-energy tail of the Lorentzians $L_{e,h}$ has been cut at an energy value $3\Gamma_e(3\Gamma_h)$ below the peak,⁹ i.e., removing about 10% of the spectral weight from their low energy tail. As shown in Fig. 3 for two typical cases, Eq. (1) gives good fits with parameter values very close to those obtained from Eq. (3). Only a detailed calculation of the spectral functions for several occupied 1D subbands at finite temperature would justify a less rough modeling, by including, for instance, energy-dependent lifetime broadenings. Actually, we find that the proposed model becomes unsatisfactory only for the spectra recorded at short delays (< 200 ps) or at very high carrier densities (having a very broad and featureless line shape).

For a very refined line-shape model, also the full dispersion of the coupled valence bands and optical matrix elements and the independent BGR of different subbands should be taken into account (as in Ref. 13 for GaAs quantum wells). However, in the investigated wide quantum wires already five transitions overlap within 50 meV above the fundamental $n_y=1$ gap. This makes difficult to get information on the BGR of the individual subbands from a simple statistical line-shape fitting. In this work we therefore concentrate on the global carrier density dependence of the BGR obtained from Eq. (3). The 1D carrier density (cm^{-1}) has been adjusted as free

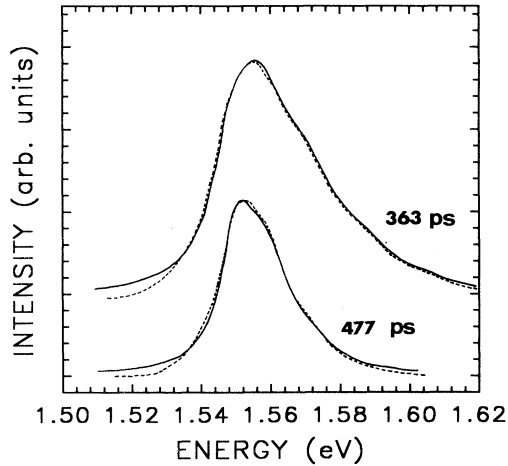


FIG. 3. Theoretical line shapes corresponding to the spectra of Fig. 1(b) for delays of 363 ps (upper part, vertically displaced by 0.5) and 477 ps (lower part): the full curves are obtained from Eq. (3) as the fits in Fig. 2 (with parameter values, respectively, $n = 1.37 \times 10^6 \text{ cm}^{-1}$, $K_B T = 11.7 \text{ meV}$, BGR = 13 meV, $\Gamma = 13.8 \text{ meV}$, and $n = 0.77 \times 10^6 \text{ cm}^{-1}$; $K_B T = 6.4 \text{ meV}$; BGR = 12.2 meV; $\Gamma = 11 \text{ meV}$), the dashed curves are obtained from Eq. (1) (with parameter values, respectively, $n = 1.39 \times 10^6 \text{ cm}^{-1}$, $K_B T = 14.4 \text{ meV}$, BGR = 12 meV, $\Gamma_e + \Gamma_h = 13.8 \text{ meV}$, and $n = 0.74 \times 10^6 \text{ cm}^{-1}$, $K_B T = 8.4 \text{ meV}$; BGR = 10.5 meV; $\Gamma_e + \Gamma_h = 11 \text{ meV}$).

parameter in the line-shape fitting. The temperature-dependent chemical potential of the EHP has been evaluated starting from the 1D carrier densities and according to the well known thermodynamic Fermi-gas theory. In Fig. 4 we show the chemical potentials of 1D electrons and holes at two temperatures and for a range of 1D $e-h$ pair densities (n) representative of the experimental conditions (continuous line). In order to evaluate the difference with respect to the 2D case, we also compare in Fig. 4 the 1D chemical potential with the corresponding quantity for the 10.6-nm quantum well from which the wires were fabricated. In this case the 2D $e-h$ pair density is given by $n/60 \text{ nm}$ (dotted line in Fig. 4). Even though several 1D subbands are occupied, significant quantitative differences with respect to the 2D case are evident.

The band-gap renormalization versus the total carrier density is shown in Fig. 5. The BGR values were obtained by subtracting the best fit E_g^* values from the unperturbed $n_y=1$ quantum wire gap previously determined ($E_g = 1.566 \text{ eV}$). The analysis was performed on the whole set of spectra excited at different power densities or detected at different delays. The BGR values range between 12 and 24 meV in the carrier density range $2 \times 10^5 < n < 4 \times 10^6 \text{ cm}^{-1}$. The accuracy in the determination of the best-fit BGR values amounts to about $\pm 10\%$ (typical error bars on the BGR, as deduced from the fit parameters, are reported in Fig. 5). The smallest BGR value obtained from the fits (about 12 meV at $2 \times 10^5 \text{ cm}^{-1}$) compares with the exciton binding energy⁶ in the investigated wires, indicating that exciton ionization occurs around this carrier density. In Fig. 5 we also plot the carrier density dependence of the BGR calculated by Kuang-Hu and Das Sarma¹⁴ for quantum wires of width 1000 and 500 Å at zero temperature. This theory

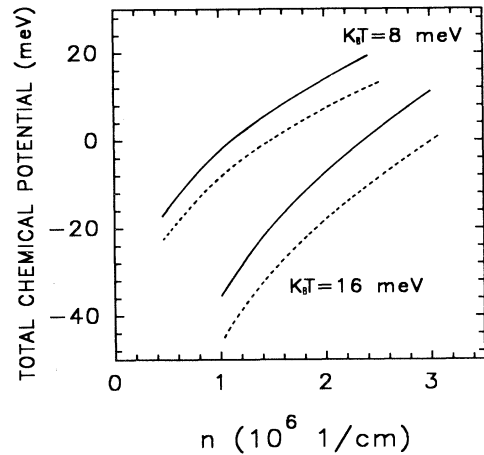


FIG. 4. The sum ($\mu_e + \mu_h$) of the chemical potentials of 1D electrons and holes measured from the bottom of the respective first quantum well 2D subbands is shown by the upper and lower full lines, respectively, for $K_B T = 16 \text{ meV}$ as a function of the 1D density of $e-h$ pairs (n). The dotted lines show the same quantity for 2D electrons and holes in the same quantum well with a 2D density of $e-h$ pairs given by $n/60 \text{ nm}$. All relevant parameters are as in the fits to the experimental spectra.

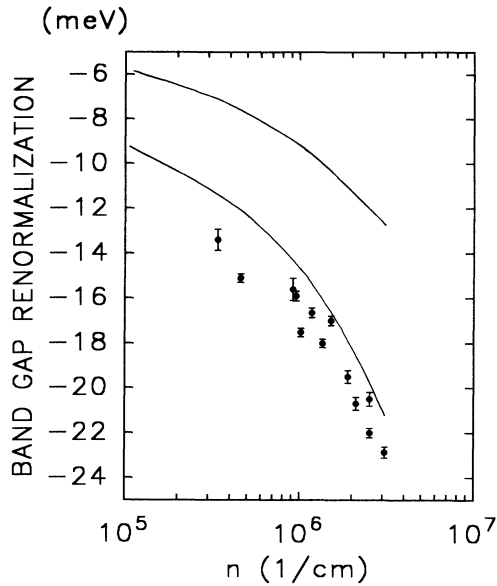


FIG. 5. Band-gap renormalization (dots) versus total carrier density obtained from the fit of the luminescence spectra under different excitation intensities and after various delays. The continuous lines are the calculated BGR curves for quantum wires of widths 1000 Å (upper curve) and 500 Å (lower curve) (after Ref. 14).

neglects the hole population and considers an electron plasma confined in the lowest conduction quantum wire subband only. Nevertheless, it is satisfactory to see that experiment and theory get close. Furthermore, our data are about 50% smaller than those predicted by Benner and Haug which were calculated for parabolic wires having a much larger subband separation than ours.¹⁵ As discussed above, though, more realistic theoretical calculations would be required for a precise comparison, between theory and experiments. Unfortunately, so far no theoretical work including the population of higher-energy subbands, and the two component EHP at finite temperature in quantum wires has been reported. We point out that the obtained carrier density dependence of the BGR is characteristic of the quasi-one-dimensional EHP. In fact, by scaling the 1D carrier density in two dimensions (by $n_{2D} = n/60 \text{ nm}$) the obtained quasi-two-dimensional BGR does not compare with the one expected for the 10.6-nm quantum well from which the wires were fabricated.¹

Now we turn to the transient behavior of the BGR. In Figs. 6(a) and 6(b) we show the temporal evolution of the total carrier density (n in cm^{-3}) and BGR obtained by the line shape fitting of the EHP luminescence excited under different power densities. As already observed in quantum wells,¹⁶ the BGR reduces at long delay times, following the decrease of the carrier density due to recombination. The initial photogenerated carrier density (short delays) depends on the intensity of the exciting pulse and shows an exponential decay. The slope of the carrier density versus time slightly increases with increasing the injected density [Fig. 6(a)], indicating some shortening of the recombination time at high carrier densi-

ty.¹⁷ However, no abrupt decrease of the recombination time due to stimulated emission is observed in the investigated quantum wires. At the lowest excitation intensity the carrier density reduces from 1.6×10^6 to $4 \times 10^5 \text{ cm}^{-3}$ in about 500 ps. Under higher excitation, the initial carrier density increases and decays following a similar time dependence. The band-gap renormalization follows this temporal evolution of the electron-hole plasma density, as shown in Fig. 6(b). The transient BGR reduces for long delays and the crystal tends to recover the original value of the unperturbed energy gap. These trends roughly indicate that a recovery time of the order of 1 ns is necessary to reform excitons originally screened by the EHP (this corresponds to the condition that BGR equals the exciton binding energy) and to resume the unperturbed energy gap of the quantum wires, under high photogeneration rates.

Finally, to complete our picture of the dynamics of the

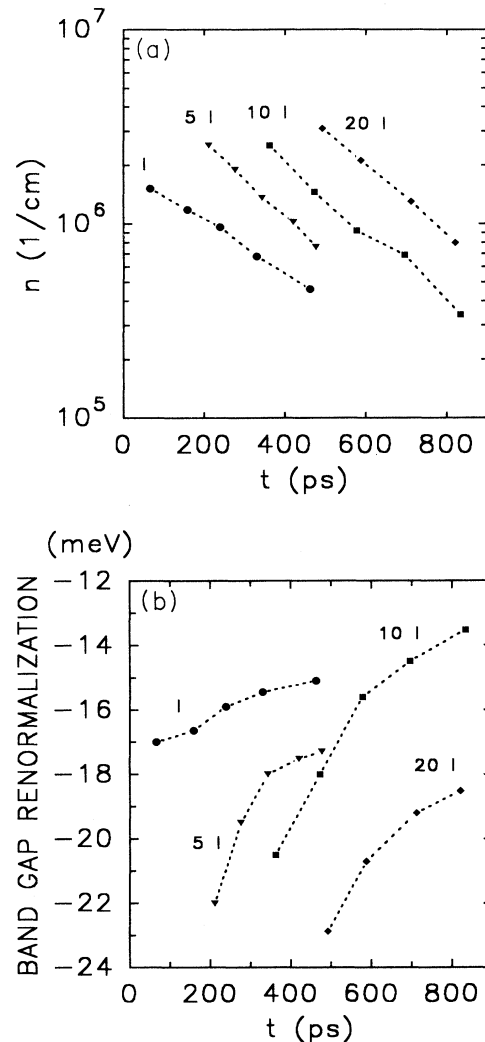


FIG. 6. Temporal evolution of the total carrier density (a) and of the band-gap renormalization (b) obtained from the fit of the time-resolved luminescence spectra under different excitation intensities ($I \approx 0.5 \text{ MW cm}^{-2}$).

EHP parameters in one dimension, we point our attention on the hot carrier cooling. In Fig. 7 we show the temporal evolution of the carrier temperature obtained for the line-shape fits of the PL spectra recorded under different injection densities. These temperatures are deduced from the Fermi-Dirac thermal distribution of the carriers in the subbands, assuming the same average temperature for the electron and hole plasmas. Within the experimental error the $K_B T$ factor follows an exponential decay in time, with a slope determined by the initial photogenerated carrier density. The average error on the best-fit $K_B T$ values amounts to $\pm 10\%$. Only at the lowest excitation intensity (I curve) the line-shape fit was reliable enough at short delays, and a $K_B T$ value of about 7.5 meV has been obtained for nominally zero delay. This value reduces to about 3 meV in approximately half nanosecond. At higher excitation intensities a very hot-carrier plasma is formed. $K_B T$ values as high as 30 meV have been obtained from the PL spectra recorded after long delays (> 250 ps). Under this condition the hot plasma regime is found to last for a time of the order of 1 ns. The $K_B T$ values reported in Fig. 7 differ by less than 10% with those obtained with the simplified line-shape model of Ref. 3. From these data we can estimate an energy loss rate for electrons and holes ranging between 7×10^{-13} and 10^{-12} W/carrier. These values, though approximated, are smaller than those expected from the calculations of Campos and Das Sarma¹⁸ valid for a 20 nm \times 20 nm wire, in the extreme quantum limit (i.e., with a single subband occupied at carrier density 10^6 cm⁻¹). Probably a theoretical treatment of the hot-carrier relaxation in the dense 1D-EHP on a time scale of 1 ns, including multisubband population and intersubband and intrasubband interactions, would be necessary to interpret our data. Subpicosecond optical experiments would be also useful to directly compare with the Monte Carlo simulation by Rota *et al.*,⁸ which analyzes the carrier re-

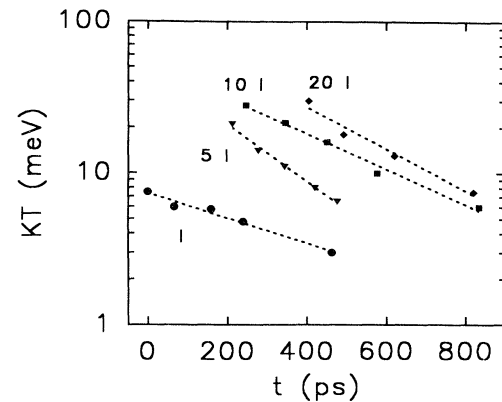


FIG. 7. Thermal energy of carriers (K_B is the Boltzmann constant and T the effective carrier temperature) as a function of time, under different excitation intensities. The dashed lines are the regression lines connecting the data points. ($I \approx 0.5$ MW cm⁻¹).

laxation of the hot EHP including electron-polar optical phonon scattering as well as electron-electron interaction for both intrasubband and intersubband transitions in quantum wires.

In conclusion, we have reported on systematic time-resolved PL measurements carried out in GaAs quantum wires under intense ps excitation. The carrier density dependence and the temporal evolution of the band-gap renormalization and carrier temperature have been determined and compared with available theories.

ACKNOWLEDGMENTS

This work was sponsored by MURST and CNR of Italy and by the NANOPT-ESPRIT project. Dipartimento di Fisica, Universita' di Bari is Unita' GNEQP.

*Permanent address: Dipartimento Scienza dei Materiali, Universita' di Lecce, via Arnesano, 73100 Lecce, Italy.

†Present address: Centro Laser S.r.L, Strada prov. Casamassima km 3, 70100 Bari, Italy.

‡Permanent address: Institute für Angewandte Physik, Jungensstrasse 11, D-2000 Hamburg 36, FRG.

§Permanent address: Paul Drude Institut FKE, Hausvogteiplatz 5-7, 0-1086-Berlin, FRG.

¹For updated reviews see: H. Kalt and M. Rinker, *Phys. Rev. B* **45**, 1139 (1992); S. Schmitt-Rink, D. S. Chemla, and D. A. B. Miller, *Adv. Phys.* **38**, 89 (1989); R. Cingolani and K. Ploog, *Adv. Phys.* **40**, 535 (1991).

²L. Tapfer, G. C. LaRocca, H. Lage, R. Cingolani, P. Grambow, D. Heitmann, A. Fisher, and K. Ploog, *Surf. Sci.* **267**, 227 (1992).

³R. Cingolani, H. Lage, L. Tapfer, H. Kalt, D. Heitmann, and K. Ploog, *Phys. Rev. Lett.* **67**, 891 (1991).

⁴Usually the actual gap of the crystal does not coincide with the energy of the peak of the high-excitation-intensity photoluminescence. Nevertheless, the spacing among the spectral peaks reflects the subband spacing quite accurately. The vertical lines in Fig. 1 have therefore been slightly shifted to show

the agreement between the calculated and experimental quantum wire subband splittings. For a more precise estimate of the gap position one has to perform a line-shape fitting.

⁵U. Bockelmann and G. Bastard, *Europhys. Lett.* **15**, 215 (1991).

⁶R. Cingolani, M. Lepore, R. Tommasi, I. M. Catalano, H. Lage, D. Heitmann, K. Ploog, A. Shimizu, H. Sakaki, and T. Ogawa, *Phys. Rev. Lett.* **69**, 1276 (1992).

⁷C. Ell, R. Blanck, S. Benner, and H. Haug, *J. Opt. Soc. Am. B* **6**, 2006 (1989).

⁸L. Rota, F. Rossi, S. M. Goodnick, P. Lugli, E. Molinari and W. Porod, *Phys. Rev. B* **47**, 1632 (1993).

⁹A. Selloni, S. Modesti, and M. Capizzi, *Phys. Rev. B* **30**, 821 (1984).

¹⁰P. T. Landsberg and D. J. Robbins, *Solid State Electron.* **28**, 137 (1985); A. Kucharska and D. J. Robbins, *IEEE J. Quantum Electron.* **26**, 443 (1990); P. T. Landsberg, M. S. Abrahams, and M. Osinski, *IEEE J. Quantum Electron.* **21**, 24 (1985).

¹¹For the series of spectra shown in Fig. 2, for instance, each spectrum has been binned to 43 channels (for a total of 172 data points for the four spectra) that have been fitted using the MINUIT code from CERN varying four parameters (n , E_g^* ,

T , and Γ) for each spectrum. Further, for each series of time-resolved spectra recorded at a certain excitation intensity, a single baseline value and a single intensity factor were taken as free parameters, the other being scaled according to the experimentally measured intensity values. This results in a value of χ^2 with 154 degrees of freedom of about 160 ($\pm 30\%$ due to uncertainties in the indetermination of the experimental error bars). These values hold for the spectra recorded with long delays or few occupied subbands. For short delays (~ 200 ps) the fits get worst.

¹²Typical best-fit values for the damping parameter $\Gamma_3 + \Gamma_h$ range between 8 and 19 meV with an average error of 15%. This compares well with those reported in recent theoretical

calculation [see, for example, R. Binder, D. Scott, A. E. Paul, M. Lindberg, K. Henneberger, and S. W. Koch, *Phys. Rev. B* **45**, 1107 (1992)].

¹³E. Lach, A. Forchel, D. A. Broido, T. L. Reineke, G. Weimann, and W. Schlapp, *Phys. Rev. B* **42**, 5395 (1990).

¹⁴Ben Yu-Kuang Hu and S. Das Sarma, *Phys. Rev. Lett.* **68**, 1750 (1992).

¹⁵S. Benner and H. Haug, *Europhys. Lett.* **16**, 579 (1991).

¹⁶R. Cingolani, H. Kalt, and K. Ploog, *Phys. Rev. B* **42**, 7655 (1990).

¹⁷E. O. Goebel, R. Hoeger, J. Kuhl, H. J. Polland, and K. Ploog, *Appl. Phys. Lett.* **47**, 781 (1985).

¹⁸V. B. Campos and S. Das Sarma, *Phys. Rev. B* **45**, 3898 (1992).